

Article

Graphene Encapsulated Silicon Carbide Nanocomposites for High and Low Power Energy Storage Applications

Emiliano Martínez-Periñán ^{1,2}, Christopher W. Foster ¹, Michael P. Down ¹, Yan Zhang ³, Xiaobo Ji ³, Encarnación Lorenzo ², Dmitrijs Kononovs ⁴, Anatoly I. Saprykin ⁵, Vladimir N. Yakovlev ⁶, Georgy A. Pozdnyakov ⁷ and Craig E. Banks ^{1,*}

¹ Faculty of Science and Engineering, Manchester Metropolitan University, Chester Street, Manchester M1 5GD, UK; emiliano.martinez@uam.es (E.M.-P.); cwfoster90@gmail.com (C.W.F.); michaeldown@hotmail.com (M.P.D.)

² Departamento de Química Analítica y Análisis Instrumental, Universidad Autónoma de Madrid, 28049 Madrid, Spain; encarnacion.lorenzo@uam.es

³ College of Chemistry and Chemical Engineering, Central South University, Changsha 410083, China; zyalj@csu.edu.cn (Y.Z.); xji.csu.edu@gmail.com (X.J.)

⁴ Adiabatic Nanotechnologies, Doma laukums 2, Riga LV-1050, Latvia; dk@adiananotech.com

⁵ Nicolaev Institute of Inorganic Chemistry, Novosibirsk State University, Novosibirsk 630090, Russia; saprykin@niic.nsc.ru

⁶ Nicolaev Institute of Inorganic Chemistry, Novosibirsk 630090, Siberian State University of Water Transport, Novosibirsk 630099, Russia; yvn@ngs.ru

⁷ Khristianovich Institute of Theoretical and Applied Mechanics, Novosibirsk State University, Novosibirsk 630090, Russia; georg@itam.nsc.ru

* Correspondence: c.banks@mmu.ac.uk; Tel.: +44-(0)161-2471-196

Received: 13 May 2017; Accepted: 12 June 2017; Published: 20 June 2017

Abstract: In this paper, a graphene decorated SiC nanomaterial (graphene@SiC) fabricated via a facile adiabatic process was physicochemically characterised, then applied as a supercapacitor material and as an anode within a Li-ion battery (LIB). The reported graphene@SiC nanomaterial demonstrated excellent supercapacitive behaviour with a relatively high power density and specific capacitance of $4800 \text{ W}\cdot\text{kg}^{-1}$ and $394 \text{ F}\cdot\text{g}^{-1}$, respectively. In terms of its capabilities as an anode within an LIB, the layered-graphene overwhelms the Li-intercalation, which is reflected in the obtained specific capacity of $150 \text{ mAh}\cdot\text{g}^{-1}$, with a columbic efficiency of $\sim 99\%$ (after 450 cycles) at a current of $100 \text{ mA}\cdot\text{g}^{-1}$.

Keywords: graphene encapsulated silicon carbide; energy storage; adiabatic synthesis

1. Introduction

With the ever-increasing ecological demand for the utilisation of renewable energy sources, such as solar and wind, the development of sustainable energy conversion and storage technologies are paramount [1–3]. One of the most successful (in terms of commercialisation) effective energy storage devices has been the lithium-ion battery (LIB). However, there needs to a rapid advancement within the research community to improve the energy storage capabilities of LIBs in order to foster a reliance upon current renewable energy systems [4]. The most common approach to improve the overall specific capacity and voltage capabilities of these LIBs is the exploration of an array of nanomaterials (as potential anodes and cathodes). These systems are effective; however, the release of stored energy in many battery applications is generally slow, as the power densities of these systems are relatively small [2,5]. Consequently, the incorporation of high-power supercapacitors is regularly applied within industry and academia, allowing for a reduced battery stress, which therefore increases

the longevity of these battery systems [6,7]. Supercapacitors are recognised as promising devices for energy applications within high-power electronics, electric vehicles, and hybrid electric vehicles, due to their capacities to produce high power density, long cycling life, and minimum charge separation [8,9]. Nonetheless, supercapacitors can only offer fast release of energy created and stored from renewable energy sources.

Over recent years, graphene-based materials have received particular attention as a potential electrode material for electrochemical energy generation and storage due to its unique morphology, relatively large specific area, high structural stability, and excellent electrical conductivity (at room temperature) [10,11]. Despite the interest in the advanced nanoscale properties of graphene, the application of the material within a large-scale production of energy storage applications is still in its primary implementation phase. This is most likely due to limitations in the availability of large-scale high-quality graphene and due to the challenge related to the transfer of graphene powders to the substrate/device location, which results in a difficult fabrication process. Numerous methods have been reported for the synthesis of graphene-like materials from gaseous, solid, and liquid precursors [12,13]. Over recent years, the synthesis of graphenes from carbides has attracted increased attention [14,15]. Carbide-derived carbons (CDCs) are a large family of carbon materials fabricated from carbide precursors that are transformed into pure carbon via physical (i.e., thermal decomposition) or chemical (i.e., halogenation) processes [14]. CDC-synthesised electrode materials allow for a high specific surface area and tunable pore size with a narrow size distribution, making them an excellent option as a supercapacitor material [16,17]. Recently, nanosized SiC has been synthesised and utilised as an anode within an LIB by Kumari et al., who reported SiC to be a very useful anode material within LIBs with a specific capacity of $1200 \text{ mAh}\cdot\text{g}^{-1}$ over 200 cycles [18]. Previously, the authors have proposed a technique to synthesise nanosized powders of silicon via the thermal decomposition of monosilane/argon mixture (1:9), using the adiabatic compression method [19] as an alternative to traditionally utilised technology for the preparation of silicon-based nanopowders via evaporation and condensation of the solids or by thermal decomposition of monosilane [20,21].

This article utilises a graphene encapsulated SiC nanopowder, graphene@SiC, fabricated via a facile adiabatic process. The proposed technology allows for the production of highly pure graphene@SiC nanopowders at a low energy consumption without the use of complex equipment, and provides a high monodispersity of the desired product in a single step methodology which is scalable. This graphene@SiC composite is employed as a supercapacitor and as a potential anode material within an LIB in order to understand/investigate its potential as a supercapacitor-LIB hybrid device that could potentially deliver high power and high energy capabilities.

2. Results and Discussion

2.1. Physicochemical Characterisation of the Graphene@SiC Nanoparticles

The graphene@SiC nanoparticles were fabricated as described in the Experimental Section and ESI. First, the surface morphology of the graphene@SiC nanopowder was explored via transmission electron microscopy (TEM). Figure 1A,B demonstrate that the diameter of the SiC particles ranged from 5 to 15 nm. Additionally, these well-defined core-shell structures were clearly encapsulated by few to multilayer graphene sheets, which was confirmed by electron diffraction imaging of the nanoparticle core (Figure S1), generating a spherical nanoparticle of ~ 10 nm in diameter with low polydispersity. Next, we analysed the surface of the nanoparticulates via scanning electron microscopy (SEM); Figure S2A,B illustrate images over increasing magnifications where it can be observed that the powder was formed of small porous grains/domains, indicating a vast surface/volume ratio. The energy dispersive X-ray analysis (EDX) demonstrated the presence of carbon (43.7 ± 1.0), oxygen (9.6 ± 0.9), and silicon (46.7 ± 0.4), indicating that the graphene structure possessed oxygen functionality. Raman characterisation of the graphene@SiC surface is depicted in Figure 1C; the peaks observed at 1324 cm^{-1} and 1589 cm^{-1} correspond to the D and G of graphene bands, respectively.

The intensity of the 2D graphene band at 2665 cm^{-1} is indicative of the presence of highly defective few to multilayer graphene sheets encapsulating the SiC [22,23].

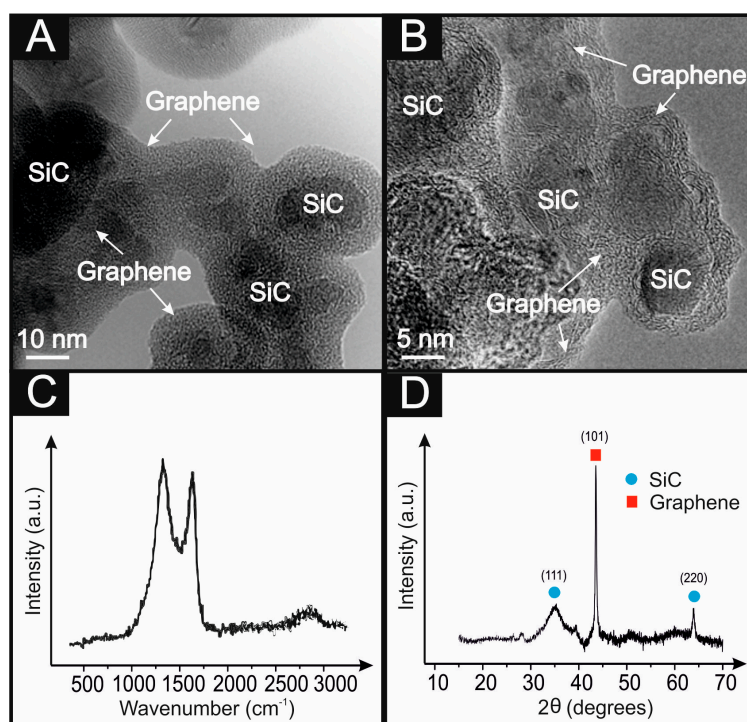


Figure 1. Transmission electron microscopy (TEM) (A,B) imaging, Raman (C), and X-ray diffraction (XRD) (D) analysis of the graphene@SiC.

To understand the crystallinity of the graphene@SiC powder, X-ray diffraction (XRD) was performed and is reported in Figure 1D, which confirms the presence of two different crystalline structures that form the graphene@SiC nanoparticles. Figure 1D illustrates a clear peak at 43° , which corresponds to the reflection of the graphene crystal plane (101) reported by the Joint Committee on Powder Diffraction Standards (JCPDS, card No. 75-1621) [24]. However, an additional smaller peak at $\sim 25^\circ$ indicates the presence of the (002) plane [24]. The presence of the two graphene crystalline orientations indicates the different orientations of graphene surrounding the core nanoparticles. SiC is also detected, showing two characteristic peaks at 64° and a peak centre at 35° associated with the reflection of the crystal planes (111) and (220), respectively [25], indicating the crystal structure of SiC and the formation of the core by different orientations of SiC as reported by JCPDS (Card No: 29-1129 and 01-072-0018). In addition to these peaks for graphene and SiC, there is a slight presence of Si (111) at 28° ; therefore, some negligible contamination of Si from the synthesis method could be possible, as the Raman spectra does not exhibit the characteristic peak of Silicon (Si-Si) typically at 520 cm^{-1} , which is a common standard within Raman measurements.

In addition, Brunauer-Emmet-Teller (BET) analysis of the powder sample exhibited an active surface of $247 \pm 10\text{ m}^2\cdot\text{g}^{-1}$, which is a typical porosity of graphene-based composites reported in the literature [26].

2.2. Graphene@SiC Capabilities as a High-Power Supercapacitor Material

The graphene@SiC nanomaterial was next explored for its potential ability to be the basis of a high-power supercapacitor material. To successfully investigate the capabilities of the graphene@SiC, the nanosized material was drop-cast onto a graphite screen-printed electrode (graphene@SiC/SPE), as described within the Experimental Section. SEM images of the homogenous distribution of the powder

over the entire electrode surface, as exhibited in Figure S2C,D, demonstrate that the graphene@SiC still maintains its powder-like structure.

Cyclic voltammetric experiments of the graphene@SiC/SPE were performed in a 1 M H₂SO₄ solution and are depicted in Figure S3, utilising 20 µg graphene@SiC/SPE, unmodified SPE, and 5% Nafion/SPE. It is clear that the SPE modified with the graphene@SiC presents a larger capacitive current than that of their unmodified counterparts. As expected, no Faradaic peaks were present within the cyclic voltammograms, illustrating a typical rectangular shape over the selected potential window (−1 to 1 V). To understand the overall effect that the graphene@SiC has upon the increased capacitive behaviour, a coverage studied was subsequently explored (5–300 µg). Figure 2A demonstrates an increase within the capacitive current upon increasing quantities of graphene@SiC utilised; intriguingly, there was no overwhelming effect upon the conductivity or any sign of reduced performance at higher coverages. The charge-discharge characteristics of any supercapacitor is vitally important, indicating that the capacitance and efficiency of these graphene@SiC/SPE devices are tested as a supercapacitor material by means of galvanostatic DC analysis, providing charge/discharge characteristics in a 1.0 M H₂SO₄ aqueous solution. Typically, the capacitance (C_{total}) of the supercapacitor is evaluated from the slope of the charge/discharge cycles, $C_{total} = \frac{I}{(dV/dt)}$ where, I is the current applied, and V is the potential measured over time, t . Figure 2B depicts the charge-discharge curves of graphene@SiC/SPE modified with increasing masses of graphene@SiC. The capacitance results are demonstrated in Figure 2B, where an increase in the overall total capacitance is demonstrated as a consequence of the increased amount of graphene@SiC on the SPE surface, demonstrating the expected behaviour due to the high conductivity of the graphene and the increased electroactive area produced by the porous structure of the material. The values for the specific capacitance of the lowest graphene@SiC modification (i.e., 5 µg graphene@SiC/SPE at 0.5 µA) was found to correspond to 394 F·g^{−1}; such values are comparable to current literature by Sarno et al. [27], who reported a capacitance of 325 F·g^{−1} utilising graphene-coated SiC.

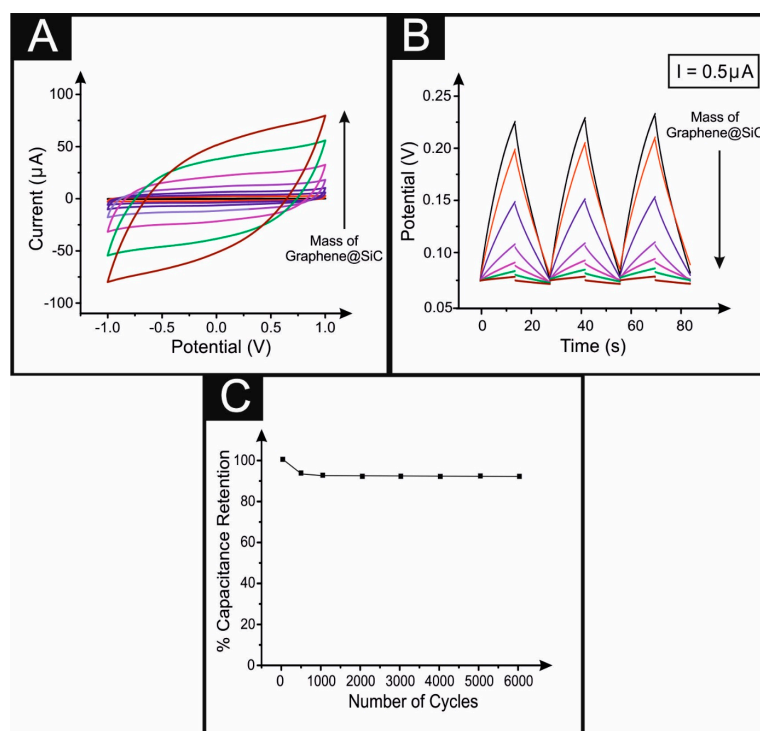


Figure 2. Cyclic voltammograms (A) and charge-discharge curves (B) of increasing masses of graphene@SiC in a 0.1 M H₂SO₄ aqueous solution. Original capacitance retention percentage vs. charge-discharge number of cycles apply (C).

The charge-discharge stability was also studied over 6000 galvanostatic cycles (Figure 2C). The capacitance retention values demonstrated that after a slight drop to 90%, the successive cycles retained the capacitance between 87% and 90% of the initial capacitance over the entire range of cycles. Typically, a supercapacitor material should exhibit a low energy density (E) and a high power density (P), the values of which are calculated using $E = I \frac{(dV)(dt)}{2m}$ and $P = I \frac{(dV)}{2m}$, respectively, where m is the mass of the graphene@SiC powder residing upon the surface of the SPE (i.e., 5 μg), in this case the values correspond to 0.02 Wh/kg and 4800 W/kg, respectively. These values are indicative of a high-power supercapacitor. A similar graphene@SiC powder was reported by Sarno et al. [27] which indicated an increased energy density, however, the (excess) time required to charge/discharge in the aforementioned study was greatly increased compared the values reported in this article [27].

2.3. Graphene@SiC Capabilities as a Li-ion Anode Material

For the first time, we investigated the capabilities of graphene@SiC as a potential anode within a Li-ion battery (LIB). The charge-discharge voltage profiles for the graphene@SiC electrode are presented in Figure 3A, in which the LIB was cycled at $100 \text{ mA}\cdot\text{g}^{-1}$ over the voltage range of 0.01–3.0 V vs. Li/Li⁺. It is clear upon inspection of Figure 3A that the voltage window was indicative of a graphite-based anode material (i.e., < 1 V vs. Li/Li⁺). Upon creation of the solid electrolyte interface (SEI) layer, the voltage capabilities remained stagnant at ~ 0.6 V, which was associated with the electrolyte decomposition and formation of lithium organic compounds. Represented within ESI Figure S4 are cyclic voltammograms for first to fifth scans of the Li-ion battery: upon the first scan a visible reduction peak was present at ~ 0.6 , indicating the intercalation of the Li-ions upon the graphitic structure, and the de-intercalation process was present at 0.25–0.45 V. It is important to note that the intensity of the redox couple became stable upon the second to fifth scans. The discharge and charge capacities were measured to be 990 and 170 $\text{mAh}\cdot\text{g}^{-1}$, respectively (Figure 3B), exhibiting a low initial coulombic efficiency of $\sim 25\%$. Nonetheless, over 10–200 cycles the overall reversibility improved and a coulombic efficiency of $\sim 99\%$ was demonstrated, at a charge and discharge capacity of 150 $\text{mAh}\cdot\text{g}^{-1}$. The rate capabilities (Figure 3C) of the graphene@SiC anode were next considered, exhibiting discharge capacities of 300, 200, 175, 150, 100, 75, and 50 $\text{mAh}\cdot\text{g}^{-1}$ at current densities of 100, 200, 400, 600, 800, 1000, and 1200 $\text{mA}\cdot\text{g}^{-1}$ respectively. Upon changing the current density back to 100 $\text{mA}\cdot\text{g}^{-1}$, the discharge capacity exhibited a recovery to $\sim 300 \text{ mAh}\cdot\text{g}^{-1}$.

While these results give an interesting output, this is far from the outcomes expected from SiC (as an anode material), which had recently been individually reported to exhibit discharge capacities between 1200 and 3750 $\text{mAh}\cdot\text{g}^{-1}$ [18,28]. Clearly, the graphene shell precluded the insertion/deinsertion of the Li-ion, hence the overall performance of the battery was limited to the shells' characteristics. To conclude, the performance of this material could be improved if the number/amount of graphene layers was reduced/controlled, potentially warranting further examination of this in the field.

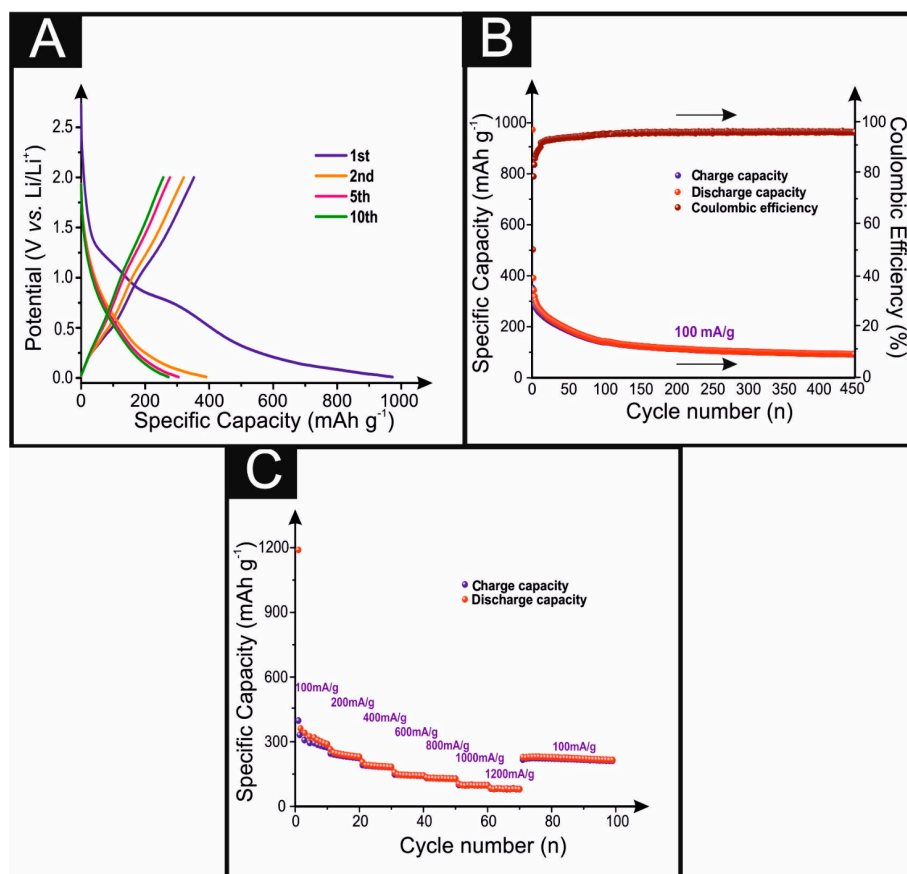


Figure 3. Charge/discharge profiles (A), cycling properties/coulombic efficiency (B), and rate capability of the graphene@SiC anode (C). These tests were carried out in batches of three, with an overall error within 10–15% of the specific capacity.

3. Experimental Section

Nafion 5% solution and pure sulfuric acid were of analytical grade and were used without any further purification from Sigma-Aldrich (Gillingham, UK). The solutions were prepared with deionized water of a resistivity no lower than 18 M Ω ·cm. Graphene@SiC nanoparticles were fabricated via a facile adiabatic based method. This approach allowed nanopowders to be obtained by initiating the synthesis of the target products via rapid and uniform temperature rises throughout the volume of a reactor, which was filled with a mixture of gaseous precursors. In this case, the adiabatic compression of a mixture of silane and acetylene (with a buffer gas) resulted in an increase in temperature above the decomposition temperatures of these reactants, leading to the synthesis of solid phase silicon carbide (SiC). The utilisation of this technology led to the synthesis of graphene@SiC nanoparticles with an average size of 10 nm in diameter, with a low polydispersity (95% monodispersity). The supporting information gives more details on the adiabatic methodology and its benefits for producing the graphene@SiC nanomaterial.

All electrochemical measurements were performed with an Autolab TYPE III (Metrohm, Kanaalweg, The Netherlands). It should be noted that the charge-discharge curves were obtained using a two-electrode configuration and the cyclic voltammetric (CV) studies were carried out utilising a three-electrode system, in which a platinum wire and saturated calomel electrode (SCE) were used as counter and reference electrodes, respectively. Graphene@SiC screen-printed electrodes (graphene@SiC/SPE) were prepared by drop-casting aliquots of a Nafion suspension containing graphene@SiC onto the screen-printed working electrode (fabrication method described within the ESI)

with a micropipette. After 30 min, the Nafion completely evaporated (at ambient temperature) and the modified electrodes were ready for use.

The morphology and structure of the graphene@SiC powder and the drop-cast electrodes were analysed via scanning electron microscopy (SEM) (JEOL JSM-840; JEOL, Welwyn Garden City, UK), equipped with an X-ray detector for the energy dispersion X-ray analysis (EDX) microanalysis. X-ray diffraction (XRD) analyses were measured with an X-ray diffractometer (Philips, Model FW 1700 series, Eindhoven, The Netherlands), used with monochromated Ni-filtered $\text{CuK}\alpha$ radiation ($\lambda = 1.54 \text{ \AA}$), and the measurements were taken at 40 kV and 30 mA, with a scanning rate of $0.06^\circ \cdot \text{min}^{-1}$ and 2 θ ranges from 15 to 70. The diffraction data was analysed using the DIFRAC plus (Evaluation Package, Bruker, Billerica, MA, USA). Raman spectroscopy was performed using an “inVia” confocal Raman microscope (Renishaw PLC, Gloucestershire, UK) equipped with a confocal microscope (50 \times objective) spectrometer with an argon laser (514 nm excitation) at a very low laser power level (0.8 mW) to avoid any heating effects. The specific surface areas for N_2 were calculated using the Brunauer-Emmet-Teller (BET) model.

CR2016-type coin cells were assembled inside a glovebox (mBraun, Dieselstr, Kronberg, Germany) ($\text{H}_2\text{O} < 0.5 \text{ ppm}$, $\text{O}_2 < 0.5 \text{ ppm}$) using a metallic lithium counter/reference electrode, a polypropylene separator (Celgard 2400, Concord, NC, USA), and an electrolyte of 1 M LiPF_6 in ethylene carbonate and dimethyl carbonate (EC–DMC, 1:1). The working electrodes were made of 70% graphene@SiC material, 15% carboxymethyl cellulose binder, and 15% Super P additive. The typical mass loading of active materials was controlled at 1.2–1.3 $\text{mg} \cdot \text{cm}^{-2}$. The coin cells were assembled in the glove box filled with highly pure argon gas (O_2 and H_2O levels $< 0.5 \text{ ppm}$). The cycling stability and rate capability measurements were conducted using an Arbin battery cycler (Arbin BT2000, College Station, TX, USA). The electrochemical properties of the cells were evaluated by cyclic voltammetry (CV) (Solartron Analytical, Ametek, Farnborough, UK).

4. Conclusions

We demonstrated, for the first time, the utilisation of a graphene encapsulated SiC nanomaterial fabricated via an adiabatic process as a potential supercapacitor material and as an anode within an LIB. The adiabatic synthetic process allowed for the production of highly pure graphene@SiC nanopowders, at a low energy consumption without the use of complex equipment, and provided a high monodispersity of desired product in a single step, scalable methodology. Moreover, as the material was inexpensive, this approach provided has clear advantages for the scale-up of these results.

It was found that the graphene@SiC nanopowders had potential for utilisation within a supercapacitor device, as they exhibited relatively high energy density and specific capacitance. In addition, the incorporation of this material as a potential anode within an LIB was explored, where it was evident that the graphene-like material dominated the overall intercalation of the Li-ions. Overall, this material could potentially be utilised within a hybrid battery-supercapacitor system if the Li-ions were allowed to intercalate with the SiC core. Therefore, future work will involve looking at the effect of varying thicknesses of graphene encapsulation upon energy storage capacities.

Supplementary Materials: The following are available online at <http://www.mdpi.com/2311-5629/3/2/20/s1>, Figure S1: electron diffraction image of n-SiC core in graphene@SiC, Figure S2: SEM images of the graphene@SiC nanocomposite (A,B) and a 5 μg graphene@SiC/SPE (C,D) at magnifications of $\times 250$ and $\times 20 \text{ k}$ respectively, Figure S3: cyclic voltammograms within a 0.1 M H_2SO_4 utilising a graphene@SiC/SPE, Nafion 5% SPE and unmodified SPE. Scan rate: $50 \text{ mV} \cdot \text{s}^{-1}$, Figure S4: cyclic voltammograms (vs. Li/Li^+) of the graphene@SiC nanomaterial within a Li-ion cell. Scan rate: $0.1 \text{ mV} \cdot \text{s}^{-1}$.

Acknowledgments: Funding from the Engineering and Physical Sciences Research Council (Reference: EP/N001877/1), British Council Institutional Grant Link (No. 172726574) and the Russian Foundation for Fundamental Research (No. 16-03-00846) is acknowledged. Emiliano Martínez-Periñán acknowledges funding from Comunidad de Madrid (NANOAVANSENS Program) for financial support.

Author Contributions: Craig E. Banks conceived the overall idea and concept. Craig E. Banks and Christopher W. Foster designed the experiments and manuscript. Emiliano Martínez-Periñán, Michael P. Down

and Encarnación Lorenzo carried out the supercapacitive electrochemical experiments. Yan Zhang and Xiaobo Ji provided battery testing and fabrication. Craig E. Banks and Christopher W. Foster interpreted all the data. Dmitrijs Kononovs, Anatoly I. Saprykin, Vladimir N. Yakovlev and Georgy A. Pozdnyakov fabricating and characterising the graphene@SiC nanopowders. All the authors have contributed to the writing of this article.

Conflicts of Interest: The authors declare no conflict of interest.

References

1. Rowley-Neale, S.J.; Brownson, D.A.C.; Smith, G.C.; Sawtell, D.A.G.; Kelly, P.J.; Banks, C.E. 2D nanosheet molybdenum disulphide (MoS₂) modified electrodes explored towards the hydrogen evolution reaction. *Nanoscale* **2015**, *7*, 18152–18168. [[CrossRef](#)] [[PubMed](#)]
2. Arico, A.S.; Bruce, P.; Scrosati, B.; Tarascon, J.-M.; van Schalkwijk, W. Nanostructured materials for advanced energy conversion and storage devices. *Nat. Mater.* **2005**, *4*, 366–377. [[CrossRef](#)] [[PubMed](#)]
3. Goodenough, J.B.; Park, K.-S. The Li-Ion rechargeable battery: A perspective. *J. Am. Chem. Soc.* **2013**, *135*, 1167–1176. [[CrossRef](#)] [[PubMed](#)]
4. Foster, C.W.; Down, M.P.; Zhang, Y.; Ji, X.; Rowley-Neale, S.J.; Smith, G.C.; Kelly, P.J.; Banks, C.E. 3D printed graphene based energy storage devices. *Sci. Rep.* **2017**, *7*, 42233. [[CrossRef](#)] [[PubMed](#)]
5. Choi, J.W.; Aurbach, D. Promise and reality of post-lithium-ion batteries with high energy densities. *Nat. Rev. Mater.* **2016**, *1*, 16013. [[CrossRef](#)]
6. Shin, D.; Kim, Y.; Seo, J.; Chang, N.; Wang, Y.; Pedram, M. Battery-Supercapacitor Hybrid System for High-Rate Pulsed Load Applications. In Proceedings of the 2011 Design, Automation & Test in Europe, Grenoble, France, 14–18 March 2011.
7. Vlad, A.; Singh, N.; Rolland, J.; Melinte, S.; Ajayan, P.M.; Gohy, J.F. Hybrid supercapacitor-battery materials for fast electrochemical charge storage. *Sci. Rep.* **2014**, *4*, 4315. [[CrossRef](#)] [[PubMed](#)]
8. Zhang, L.L.; Zhao, X.S. Carbon-based materials as supercapacitor electrodes. *Chem. Soc. Rev.* **2009**, *38*, 2520–2531. [[CrossRef](#)] [[PubMed](#)]
9. Shao, Y.; El-Kady, M.F.; Wang, L.J.; Zhang, Q.; Li, Y.; Wang, H.; Mousavi, M.F.; Kaner, R.B. Graphene-based materials for flexible supercapacitors. *Chem. Soc. Rev.* **2015**, *44*, 3639–3665. [[CrossRef](#)] [[PubMed](#)]
10. Weiss, N.O.; Zhou, H.; Liao, L.; Liu, Y.; Jiang, S.; Huang, Y.; Duan, X. Graphene: An emerging electronic material. *Adv. Mater.* **2012**, *24*, 5782–5825. [[CrossRef](#)] [[PubMed](#)]
11. Choi, H.-J.; Jung, S.-M.; Seo, J.-M.; Chang, D.W.; Dai, L.; Baek, J.-B. Graphene for energy conversion and storage in fuel cells and supercapacitors. *Nano Energy* **2012**, *1*, 534–551. [[CrossRef](#)]
12. Bhuyan, M.S.A.; Uddin, M.N.; Islam, M.M.; Bipasha, F.A.; Hossain, S.S. Synthesis of graphene. *Int. Nano Lett.* **2016**, *6*, 65–83. [[CrossRef](#)]
13. Gadipelli, S.; Guo, Z.X. Graphene-based materials: Synthesis and gas sorption, storage and separation. *Prog. Mater. Sci.* **2015**, *69*, 1–60. [[CrossRef](#)]
14. Presser, V.; Heon, M.; Gogotsi, Y. Carbide-derived carbons—From porous networks to nanotubes and graphene. *Adv. Funct. Mater.* **2011**, *21*, 810–833. [[CrossRef](#)]
15. Hoffman, E.N.; Yushin, G.; Barsoum, M.W.; Gogotsi, Y. Synthesis of carbide-derived carbon by chlorination of Ti₂AlC. *Chem. Mater.* **2005**, *17*, 2317–2322. [[CrossRef](#)]
16. Simon, P.; Gogotsi, Y. Materials for electrochemical capacitors. *Nat. Mater.* **2008**, *7*, 845–854. [[CrossRef](#)] [[PubMed](#)]
17. Chmiola, J.; Yushin, G.; Gogotsi, Y.; Portet, C.; Simon, P.; Taberna, P.L. Anomalous increase in carbon capacitance at pore sizes less than 1 nanometer. *Science* **2006**, *313*, 1760. [[CrossRef](#)] [[PubMed](#)]
18. Kumari, T.S.D.; Jeyakumar, D.; Kumar, T.P. Nano silicon carbide: A new lithium-insertion anode material on the horizon. *RSC Adv.* **2013**, *3*, 15028–15034. [[CrossRef](#)]
19. Pozdnyakov, G.A.; Yakovlev, V.N.; Saprykin, A.I. Production of nanosized silicon powders by monosilane decomposition in an adiabatic process. *Dokl. Phys. Chem.* **2014**, *456*, 67–70. [[CrossRef](#)]
20. Umezū, I.; Takata, M.S.A. Surface hydrogenation of silicon nanocrystallites during pulsed laser ablation of silicon target in hydrogen background gas. *J. Appl. Phys.* **2008**, *103*, 114309. [[CrossRef](#)]
21. Wiggers, H.; Starke, R.; Roth, P. Silicon particle formation by pyrolysis of silane in a hot wall gasphase reactor. *Chem. Eng. Technol.* **2001**, *24*, 261–264. [[CrossRef](#)]

22. Eda, G.; Chhowalla, M. Chemically derived graphene oxide: Towards large-area thin-film electronics and optoelectronics. *Adv. Mater.* **2010**, *22*, 2392–2415. [[CrossRef](#)] [[PubMed](#)]
23. Brownson, D.A.C.; Varey, S.A.; Hussain, F.; Haigh, S.J.; Banks, C.E. Electrochemical properties of CVD grown pristine graphene: Monolayer- vs. quasi-graphene. *Nanoscale* **2014**, *6*, 1607–1621. [[CrossRef](#)] [[PubMed](#)]
24. Rao, C.N.R.; Biswas, K.; Subrahmanyam, K.S.; Govindaraj, A. Graphene, the new nanocarbon. *J. Mater. Chem.* **2009**, *19*, 2457–2469. [[CrossRef](#)]
25. Shih, C.; Rohbeck, N.; Gopalakrishnan, K.; Tulenko, J.S.; Baney, R.H. Mechanical properties and XRD studies of silicon carbide inert matrix fuel fabricated by a low temperature polymer precursor route. *J. Nucl. Mater.* **2013**, *432*, 152–159. [[CrossRef](#)]
26. Kim, H.; Park, K.-Y.; Hong, J.; Kang, K. All-graphene-battery: Bridging the gap between supercapacitors and lithium ion batteries. *Sci. Rep.* **2014**, *4*, 5278. [[CrossRef](#)] [[PubMed](#)]
27. Sarno, M.; Cirillo, C.; Scudieri, C.; Polichetti, M.; Ciambelli, P. Electrochemical applications of magnetic core-shell graphene-coated FeCo nanoparticles. *Ind. Eng. Chem. Res.* **2016**, *55*, 3157–3166. [[CrossRef](#)]
28. Shiratani, M.; Kamataki, K.; Uchida, G.; Koga, K.; Seo, H.; Itagaki, N.; Ishihara, T. SiC nanoparticle composite anode for Li-Ion batteries. *MRS Proc.* **2014**, *1678*, 8–58. [[CrossRef](#)]



© 2017 by the authors. Licensee MDPI, Basel, Switzerland. This article is an open access article distributed under the terms and conditions of the Creative Commons Attribution (CC BY) license (<http://creativecommons.org/licenses/by/4.0/>).